Accurate Treatment of Arbitrarily Shaped Dielectric Materials in the Finite Integration Technique

Stefan Kirsch[1], Lilli Kuen[1], and Rolf Schuhmann[1], *Member, IEEE*

[1]Technische Universität Berlin, Fachgebiet Theoretische Elektrotechnik, Einsteinufer 17, 10587 Berlin, Germany
{kirsch,kuen,schuhmann}@tet.tu-berlin.de

The Finite Integration Technique usually relies on a Cartesian mesh system whose planar facets in general don't coincide well with the simulated structure's material interfaces. This causes the simulation's error to be relatively high and, furthermore, degrades the method's convergence rate. This contribution proposes a generalized formula for representing the actual structure's material distribution on a discrete mesh system without compromising accuracy. In a second step, approaches to utilize the technically challenging generalized formula for practically relevant applications are demonstrated.

***Index Terms*—Convergence of Numerical Methods, Finite Volume Methods, Iterative Algorithms, Numerical Simulation**

I. Introduction

MESH BASED simulation methods generally require the simulated object's geometry and material distribution to be discretized in order to obtain a finite number of unknowns to solve for. Finite Element methods typically utilize an unstructured tetrahedral mesh that adapts well to material discontinuities. The Finite Integration Technique (FIT) [1], on the other hand, is known to offer less geometrical flexibility, because it is usually applied to structured hexahedral meshes and, hence, causes the object to be represented less accurate. In many cases, it is still competitive or even superior nevertheless, due to fast and efficient algorithms that result from the structured mesh approach.

Despite its computational efficiency, it is highly desirable to be able to use the Finite Integration Technique for arbitrarily shaped objects without introducing an error that would deteriorate the otherwise achievable second order convergence rate [2]. Various attempts have been made in order to mitigate this error. For interfaces to perfect electric conductor for example, a technique to retain the numerical method's original convergence rate is well-established [3],[4]. For dielectric interfaces, on the other hand, ongoing research has not yet culminated in a method as efficient and at the same time robust as [3],[4]. The most promising approaches rely on an artificial anisotropic material tensor ([5], [6]). A study on methods based on a priori known field behavior can be found in [7].

This work takes a theoretical approach on accurately defining a generalized material parameter in the scope of the Finite Integration Technique. Afterwards, different ways of applying it in practice are described and preliminary results promise a very beneficial outcome compared to conventional methods.

II. Finite Integration Technique

By evaluating the integral form of Maxwell's equations on a staggered grid system consisting of a primary (G) and a dual ($\widetilde{G}$) mesh (cf. Fig. 1), a matrix-vector formulation can be derived:

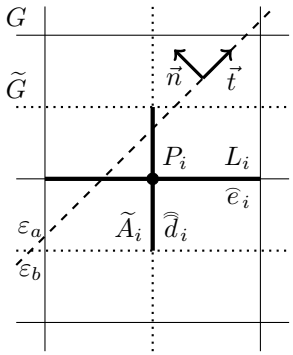

Fig. 1. Portion of a staggered Cartesian grid system (G: primary mesh, $\widetilde{G}$: dual mesh) with material interface (dashed line).

$$\mathbf{C}\widehat{\mathbf{e}} = -\frac{\mathrm{d}}{\mathrm{d}t}\widehat{\widetilde{\mathbf{b}}}, \qquad \widetilde{\mathbf{S}}\widehat{\widetilde{\mathbf{d}}} = \mathbf{q} \tag{1}$$

$$\widetilde{\mathbf{C}}\widehat{\mathbf{h}} = \frac{\mathrm{d}}{\mathrm{d}t}\widehat{\widetilde{\mathbf{d}}} + \widehat{\widetilde{\mathbf{j}}}, \qquad \mathbf{S}\widehat{\widetilde{\mathbf{b}}} = \mathbf{0} \tag{2}$$

For a detailed explanation of the symbols and their relationship cf. [1]. The electric grid voltage vector $\widehat{\mathbf{e}}$ contains the electric field integrated along each primary edge L_i. The corresponding electric grid flux is obtained by integrating the electric displacement $\vec{D}$ over the dual facet $\widetilde{A}_i$:

$$\widehat{e}_i = \int_{L_i} \vec{E} \cdot \mathrm{d}\vec{s}, \qquad \widehat{\widetilde{d}}_i = \iint_{\widetilde{A}_i} \vec{D} \cdot \mathrm{d}\vec{A} \tag{3}$$

Similar to the well-known identity $\vec{D} = \varepsilon\vec{E}$, there exists a relationship between electric grid voltages and fluxes, which can be expressed by means of a diagonal matrix $\mathbf{M}_\varepsilon$:

$$\widehat{\widetilde{\mathbf{d}}} = \mathbf{M}_\varepsilon \widehat{\mathbf{e}} \tag{4}$$

In order to derive a closed form expression for $\mathbf{M}_\varepsilon$, its ith main diagonal entry is evaluated using (3):

$$M_{\varepsilon,i} = \frac{\widehat{\widetilde{d}}_i}{\widehat{e}_i} = \frac{\iint_{\widetilde{A}_i} \vec{D} \cdot \mathrm{d}\vec{A}}{\int_{L_i} \vec{E} \cdot \mathrm{d}\vec{s}} \tag{5}$$

III. Generalized Material Averaging

Described in detail in [8] and also from a different perspective in [9], (5) can be reasonably approximated by

$$M^{\angle}_{\varepsilon,i} = \frac{\widetilde{A}_i}{L_i} \frac{\langle\varepsilon\rangle_{\widetilde{A}_i} \vec{e}_\xi \cdot \vec{E}_\mathrm{t}|_{P_i} + \vec{e}_\xi \cdot \vec{D}_\mathrm{n}|_{P_i}}{\vec{e}_\xi \cdot \vec{E}_\mathrm{t}|_{P_i} + \langle\varepsilon^{-1}\rangle_{L_i} \vec{e}_\xi \cdot \vec{D}_\mathrm{n}|_{P_i}} \tag{6}$$

for a two-dimenional computational domain. The primary edge's direction (x, y or z) has to be substituted for ξ and $\langle\varepsilon\rangle_{\widetilde{A}_i}$ stands for the permittivity's mean value over the dual area $\widetilde{A}_i$, while $\langle\varepsilon^{-1}\rangle_{L_i}$ is the inverse permittivity's mean along the primary edge L_i. $\vec{E}_\mathrm{t}|_{P_i}$ and $\vec{D}_\mathrm{n}|_{P_i}$ represent the tangential field and normal displacement evaluated at the intersection point of primary edge and dual facet P_i (cf. fig. 1). This local approximation will be shown to enable the global algorithm to maintain its second order convergence rate, even if the material interface is not aligned with any of the mesh's facets.

Under certain conditions, (6) approximates to one of the following expressions, that are well-established [7]:

$$M^{\parallel}_{\varepsilon,i} = \frac{\widetilde{A}_i \langle\varepsilon\rangle_{\widetilde{A}_i}}{L_i}, \qquad M^{\perp}_{\varepsilon,i} = \frac{\widetilde{A}_i}{L_i \langle\varepsilon^{-1}\rangle_{L_i}} \tag{7}$$

In particular, if the interface is parallel to the ξ-directed edge, the dot product $\vec{e}_\xi \cdot \vec{D}_\mathrm{n}|_{P_i}$ vanishes, $\vec{e}_\xi \cdot \vec{E}_\mathrm{t}|_{P_i}$ cancels out and $M^{\parallel}_{\varepsilon,i}$ results. Analogously, $M^{\perp}_{\varepsilon,i}$ follows for a perpendicular interface. The same happens if either the tangential electric field or the normal displacement vanish at the interface, which is also predicted by [7].

Because all these cases are incorporated, (6) can be considered a generalized material averaging formula, which, however, has a significant disadvantage compared to its simplifications. It depends on the electric field and displacement, which disables it from being calculated in preprocessing directly. The following section describes two methods of applying it to practical simulations anyway.

IV. Application

A. Iterative Approach

The problem that (6) requires knowledge of the fields that are yet to be simulated can be circumvented by an initial solution, that is obtained based on one of the expressions from (7). Assuming that this solution is reasonably accurate, the required field information is extracted and incorporated in (6). The solver is then started again, yielding an even more accurate solution than the initial one. This process is repeated iteratively until the solution has converged in a meaningful sense.

B. Non-Diagonal Material Matrix

In order to avoid solving several times, the necessary fields can be implicitly integrated in the material matrix $\mathbf{M}^{\parallel}_{\varepsilon}$. For that purpose $\widehat{e}_i$ itself and a number of neighboring grid voltages are investigated by means of their approximations represented by the denominator of (6). Assuming that $\vec{E}_\mathrm{t}|_{P_i}$ and $\vec{D}_\mathrm{n}|_{P_i}$ are constant over the small area spanned by the grid voltages taken into account, this yields a set of equations describing each grid voltage's dependence on $\vec{E}_\mathrm{t}|_{P_i}$ and $\vec{D}_\mathrm{n}|_{P_i}$. Solving this overdetermined system of equations in a least squares sense and inserting the solution into the nominator of (6) gives an explicit relation between the grid flux $\widehat{\widetilde{d}}_i$ and its corresponding, as well as its surrounding, grid voltages. This relation can be interpreted as a local material matrix, which contributes one row of the global material matrix $\mathbf{M}^{\angle}_{\varepsilon}$. Consequently, this matrix is no longer diagonal and, furthermore, not symmetric.

Note, that the above approaches are not specifically linked to a certain kind of solver. Until now, they have been successfully applied for solving 2D and 3D Maxwell's equations in the electrostatic regime and in the resonant time harmonic case. The investigated material interfaces were chosen to be smooth in order to avoid cases that require special treatment. Preliminary results (cf. fig. 2) demonstrate the generalized material averaging formula's effectiveness by means of a convergence analysis. The depicted graphs represent the relative error of an electrostatics solver compared to a known reference solution.

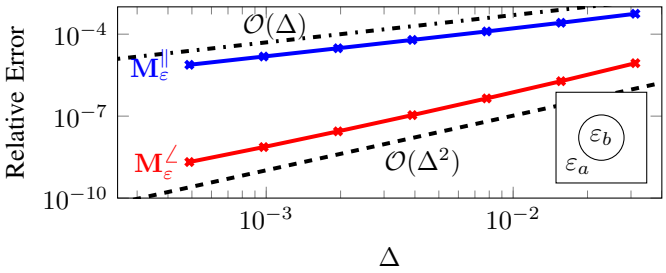

Fig. 2. Relative error of an electrostatics solver in dependence of the mesh step size Δ.

In case of the conventional material averaging procedure this error clearly converges only linearly with respect to the mesh step size Δ, as expected. The generalized approach, on the other side, not only reduces the error significantly, but also retains a convergence rate of second order.

V. Acknowledgment

The authors wish to thank Christoph Classen for fruitful discussions on this topic.

References

[1] T. Weiland. Time domain electromagnetic field computation with finite difference methods. *Int. J. Numer. Model. El.*, 9:295–319, 1996.

[2] A. Ditkowski et al. Convergent Cartesian grid methods for Maxwell's equations in complex geometries. *J. Comput. Phys.*, 170: 39–80, 2001

[3] S. Dey and R. Mittra. A locally conformal finite-difference time-domain (FDTD) algorithm for modeling three-dimensional perfectly conducting objects. *IEEE Microwave and Guided Wave Lett.*, 7:273–275, 1997.

[4] Krietenstein et al. The perfect boundary approximation technique facing the big challenge of high precision field computation. *Proceedings of the XIX Intl. Linear Accelerator Conference (LINAC), Chicago, USA*, 1998.

[5] A. Farjadpour et al. Improving accuracy by subpixel smoothing in the finite-difference time domain. *Optics Letters*, 31:2972–2974, 2006.

[6] C. A. Bauer et al. A second-order 3D electromagnetics algorithm for curved interfaces between anisotropic dielectrics on a Yee mesh. *J. Comput. Phys.*, 230:2060–2075, 2011.

[7] C. Classen et al. Local approximation based material averaging approach in the finite integration technique. *IEEE Trans. Magn.*, 48:447–450, 2012.

[8] S. Kirsch et al. A material averaging scheme for the finite integration technique based on local field information. *10th Intl. Conference on Scientific Computing in Electrical Engineering (SCEE)*, Wuppertal, Germany, 2014.

[9] M. Schauer. Ein Beitrag zur Simulation statischer und niederfrequenter Felder in nichtlinearen und hochpermeablen Materialien. PhD thesis, TU Darmstadt, 2005